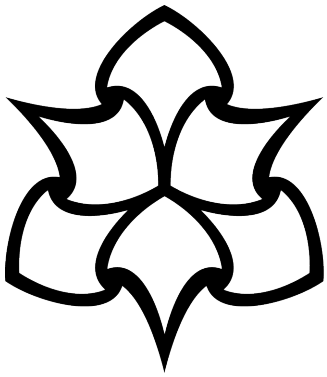

energies

MDPI

Article

Synergistic Catalytic Effect of Sulphated Zirconia—HCl System for Levulinic Acid and Solid Residue Production Using Microwave Irradiation

George Hurst [1], Juan Maria González-Carballo [2], Lubomira Tosheva [1] and Silvia Tedesco [1,*]

[1] Faculty of Science and Engineering, Manchester Metropolitan University, Chester Street, Manchester M1 5GD, UK; george.hurst2@stu.mmu.ac.uk (G.H.); l.tosheva@mmu.ac.uk (L.T.)
[2] Drochaid Research Services Ltd., Purdie Building, North Haugh, St Andrews Fife KY16 9ST, UK; juanmaria.gonzalezcarballo@drochaidresearch.com
* Correspondence: s.tedesco@mmu.ac.uk

Abstract: The synergistic conversion of *Miscanthus x Giganteous* with sulphated zirconia and dilute hydrochloric acid was investigated. The sulphated zirconia was prepared using H_2SO_4 impregnation and characterised using X-ray Diffraction (XRD), Energy-dispersive X-ray (EDX), Scanning Electron Miscroscope (SEM) spectroscopy and nitrogen adsorption–desorption measurements. The microwave-assisted reaction was evaluated at various temperatures, reaction times and catalyst-to-biomass ratios, with and without the presence of trace HCl in the solution medium for the conversion of *Miscanthus x Giganteous* to levulinic acid. The highest levulinic acid yield of 63.8% was achieved at 160 °C, 80 min and a 2:1 catalyst-to-biomass ratio, with 10 mM HCl. The catalyst recyclability was investigated with and without calcination, finding that significant humin deposition on the catalyst surface likely caused catalyst deactivation. The post-reaction solid residue was also characterised using SEM, EDX, XRD, elemental composition and nitrogen adsorption–desorption measurements. Findings indicate that this residue could potentially be used as a soil amendment or as a fuel source. The synergistic conversion of real lignocellulosic biomass with sulphated zirconia and trace hydrochloric acid showed remarkable promise and should be investigated further.

Keywords: microwave catalysis; sulphated zirconia; heterogeneous catalysis; lignocellulosic biomass; levulinic acid; hydrochars

Citation: Hurst, G.; González-Carballo, J.M.; Tosheva, L.; Tedesco, S. Synergistic Catalytic Effect of Sulphated Zirconia—HCl System for Levulinic Acid and Solid Residue Production Using Microwave Irradiation. *Energies* **2021**, *14*, 1582. https://doi.org/10.3390/en14061582

Academic Editors: Olawole Kuti and Daniel T. Hallinan, Jr.

Received: 22 February 2021
Accepted: 9 March 2021
Published: 12 March 2021

1. Introduction

Increasing concerns over serious climate change issues are currently shifting the research focus in sustainable circular economy towards the development of cleaner alternative renewable feedstocks for the production of low-carbon chemicals and energy. The production of renewable biochemicals is a pressing necessity for the manufacture of a range of low-carbon materials essential to modern life, ranging from pharmaceuticals to plastics. Lignocellulosic biomass, which is among the most abundant renewable energy resources, has received significant attention in recent years for the production of biochemicals and materials [1–3]. Non-edible cellulosic feedstocks are highly desirable substitutes for fossil resources, due to their carbon-neutral circular framework and ability to be converted into a broad range of platform chemicals. Among the top target chemical building blocks is levulinic acid (LA) [4], which can be produced by acid-catalysed dehydration of cellulose and sugars, in a single-stage process, as shown in Figure 1 [5,6]. LA is a C5 keto-acid, exhibiting both carboxylic acid and ketone functionality that can be upgraded by several routes into γ-valerlatcone, methyltetrahydrofuran and 1–4-pentanediol, among others [7–9]. Alongside mineral acids, several inorganic salts such as $FeCl_3$ have been investigated at lab scale for the production of levulinic acid from cellulose [10,11]. Recently, several commercial pilot plants have been built using mineral acid catalysts,

such as sulphuric acid, to produce LA; however, the estimated production costs have varied significantly between USD 1 and USD 8 per kilogram [12–15]. Despite their simplicity and high LA yields, utilisation of mineral acids has been associated with reactor corrosion, limited catalyst recovery and waste by-product yields, such as humins [2].

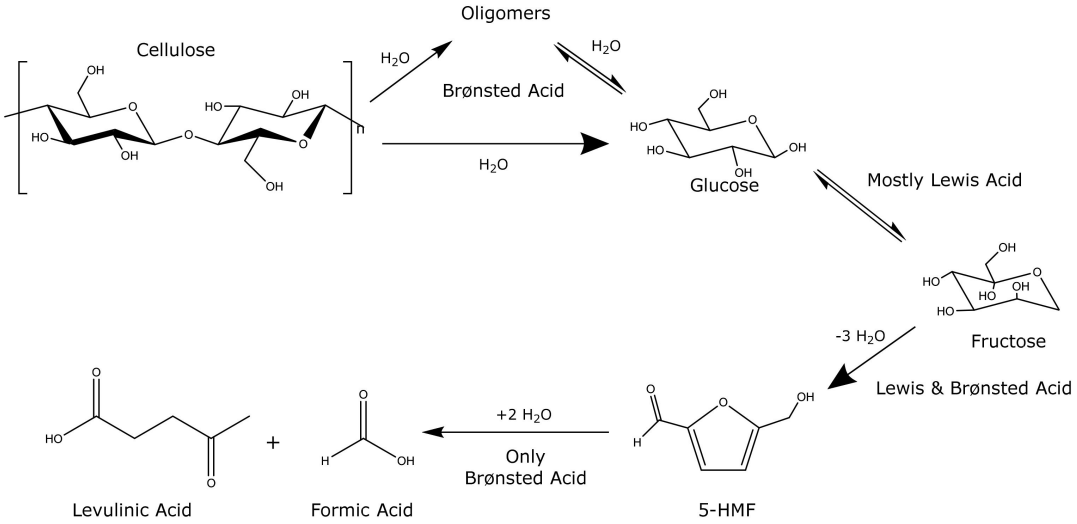

Figure 1. Formation of levulinic acid from cellulose.

Heterogeneous solid acid catalysts have been proposed by several studies [16–18] as replacements for H_2SO_4 and HCl mineral acids. Solid acid catalysts can significantly reduce equipment corrosion, lower the environmental impact and offer a more cost-effective catalyst separation method. Production of LA from monosaccharide sugars (e.g., glucose and fructose) and cellulose has been extensively studied with theoretical LA yields in excess of 50% with a broad range of solid acid catalysts including ion-exchange resins, metal oxides and modified zeolites [17,19,20]. The acidic properties of some metal oxides can be further increased by sulphate doping in order to increase and tailor the number of Brønsted and Lewis acid sites, in order to catalyse each step of the levulinic acid formation mechanism shown in Figure 1 [21]. Additionally, widely used solid acids such as sulphated zirconia (SZR) catalyse the formation of LA from lignocellulose at significantly lower catalyst concentrations than mineral acids [22,23]. SZR displays both Lewis and Brønsted acidities, which are required for glucose isomerisation to fructose and subsequent dehydration to 5-HMF, respectively. SZR has been reported to convert both simple and complex carbohydrates into 5-HMF at high rates, 30–62% and 98% yields, respectively, as well as exhibiting great LA conversion rates from cellulose [24,25].

However, the conversion of solid lignocellulosic biomass with heterogeneous catalysts has resulted in significantly lower LA yields compared with monosaccharide sugars (e.g., glucose and fructose), primarily due to the limited solid–solid interaction. Recent studies by Pyo et al. [26] attempted to promote solid acid catalysts with glucose by the addition of aqueous salts for the production of LA. Meanwhile, Kobayashi et al. reported that the addition 13 mM HCl increased the rate of hydrolysis of cellulose to glucose from 31% to 82% with a carbonaceous solid acid catalyst [27]. Geboers et al. similarly reported that trace HCl can hydrolyse solid cellulose towards soluble oligosaccharides, which can be adsorbed by the solid catalyst [28] and can more easily interact with the solid acid catalyst, reducing the solid–solid interaction bottleneck. As the efficient conversion of monosaccharides towards LA with ZrO_2 has been previously reported, the synergism with trace HCl could potentially increase LA yields with real lignocellulosic biomass.

Furthermore, commercial large-scale LA production requires full valorisation of all by-products, including hemicellulose-derived furfural, formic acid and solid residues (also known as humins) [29]. Furfural and formic acid can be separated and sold into

established commercial markets. However, the solid residues have been both under-characterised and unexplored for potential commercial applications. Works by Patil et al. and Zandvoort et al. [30,31] investigated the formation mechanisms leading to humin formation from sugars, concluding the humin residues are primarily interlinked furanic polymers. Several authors have attempted to minimise the solid residue by-product but found that residue formation cannot be avoided [31,32], although polymerisation inhibitors can reduce excessive humin formation, but not eliminate it [33] since the solid residue from lignocellulosic biomass will also contain lignin, waxy polymers and other inert fractions. Argarwal et al. and Melligan et al. [34,35] investigated its pyrolysis which resulted in low yields of phenol-rich bio-oil, 10–20 wt.%, though it requires the further development of pyrolysis technology. Furan-derived humin residues were found to form excellent building material composites; however, this a relatively low-value application [36]. Due to the high heating value (HHV), several studies have suggested the utilisation of the solid residue as a fuel source for internal energy generation [22]; however, they found this significantly increases the overall plant CO_2 emissions, reducing green credentials for producing a renewable bio-chemical. Recently, there has been growing interest in the use of chars and other carbonaceous residues as soil improvement to remedy drastically decreasing soil carbon levels [37–39]. The land application of the solid residue would not only provide a possible low-carbon emission valorisation method but could potentially alleviate a significant ecological issue, particularly for intensive agronomic systems.

In this study, we investigate the use of sulphated zirconium dioxide as a heterogeneous catalyst for the production of LA from a lignocellulosic energy crop, *Miscanthus x Giganteus*. *Miscanthus x Giganteus* was chosen as an example lignocellulosic feedstock in this study due to its high hexose content, low fertiliser requirements and widespread growing capacity, which make it among the most promising energy crops [40]. This included the investigation of the addition of dilute 10 mM HCl and optimisation of the reaction conditions for maximised yield and quantification of solid residues as well as characterisation for their potential applications.

2. Materials and Methods

2.1. Materials and Catalyst Preparation

The sulphated zirconium dioxide (SZR) catalyst was prepared using commercial $Zr(OH)_4$ (Sigma Aldrich 97%) suspended in a 0.5 M solution of H_2SO_4 under vigorous stirring for 1 h. The solid was then filtered, dried at 110 °C for 12 h and calcined at 550 °C for 3 h. Analytical-grade trace metal hydrochloric acid was purchased from Fisher-Scientific and levulinic acid, 5-HMF and furfural were purchased from Sigma Aldrich to prepare HPLC standards. *Miscanthus x Giganteus* was acquired from a local supplier, ball-milled through a 0.2 mm mesh (Retsch, ZM500), dried at 105 °C until constant weight was achieved and then stored under airtight conditions until use. The water-soluble extractives were determined using a solvent extractor (Dionex, ASE 350) with demineralised water according to NREL/TP-510-42619 [33]. The structural sugars were characterised according to NREL methods [34]. The obtained compositions (on an oven-dry basis wt.%) were 1.82% ± 0.02 ash, 5.33% ± 0.28 total extractives, 17.95% ± 0.14 Klason lignin, 38.86% ± 0.42 cellulose (glucan) and 24.08% ± 0.73 hemicelluloses. The cellulose crystallinity was determined by the peak difference method using X-ray diffraction (XRD) on a dry weight basis.

2.2. Physical Characterisation of Catalyst and Solid Residue (SR)

The compositional analysis of the catalyst surface was conducted through energy-dispersive X-ray spectroscopy (EDX), utilising an AMETEK EDAX TSL. The crystallographic phases of the catalyst were analysed with the X-ray diffraction PANalytical X'Pert Powder system, operated at 40 mA and 45 kV. The residual cellulose crystallinity in the solid residue was determined according to the method described in Section 2.1. Scanning electron microscopy (SEM) images were obtained with a Zeiss Supra 40 VP-FEG-SEM, Germany. The specific surface areas of the samples (catalyst and solid residue) were deter-

mined with a Micromeritics ASAP2020 surface area analyser. Samples were degassed for 12 h at 150 °C prior to analysis and surface areas were calculated from nitrogen adsorption data at −196 °C in the range of relative pressures between 0.05 and 0.3 using the BET model. Total pore volumes were determined from the measurements at p/p_0 of 0.99 using a density conversion factor of 0.001547. External surface areas and micropore areas were determined by the t-lot method. Pore size distributions were calculated based on the Barrett, Joyner and Halenda (BJH) model from the adsorption branch of the isotherms. Temperature-programmed desorption of ammonia (NH3-TPD) was carried out on a Micromeritics 2920 instrument, which was equipped with a TCD detector and coupled to a Balzers Thermostar quadrupole mass spectrometer. The sample, ~80 mg, was pretreated under a flow of 50 mL/min argon at 120 °C (5 °C/min) for 30 min and then at 500 °C (5 °C/min) for 20 min. The sample was then cooled down to 100 °C, and the argon flow was switched to 5%NH_3/H_2 and allowed to interact for 1 h at 100 °C. Then, the system was flushed with helium (before starting the TPD experiment). The sample was heated up to 500 °C (10 °C/min) and the effluent gas was monitored by MS and TCD. Acidity was measured based on the TCD detector signal.

2.3. Microwave Catalysis and Experimental Method

The biomass catalysis reactions were conducted using a CEM Mars 5 microwave reactor (10 mL working volume) operating at 2.45 GHz. For each experiment, the reactor was loaded with a fixed biomass amount of 0.25 g, with a varying catalyst-to-biomass ratio (0, 0.4, 1.0 or 2.0). The reaction medium was aqueous with either 10 mL of deionised water or pre-prepared 10 mM HCl. The microwave temperature was controlled via infrared measurement. The reaction temperature and time varied between 140 and 200 °C and 30–120 min, respectively. Post-reaction, the solid residue was washed with 200 mL of deionised water and separated using vacuum filtration with pre-dried and pre-weighed 2 µm filter papers before drying at 60 °C for 24 h, prior to characterisation as described in Section 2.1. The liquid fraction was subsequently filtered through a 0.2 µm filter and frozen for carbohydrate and organic acid product analysis. Levulinic acid and platform chemical concentration was quantified using an HP-1100 HPLC, equipped with an Aminex HPX-87H organic acids column, and a UV detector (λ = 226 nm). The theoretical levulinic acid yield was calculated on a dry cellulose content only basis and is presented in theoretical mol%.

2.4. Solid Residue Separation and Characterisation

The dried post-reaction solids were separated by size using 68 and 125 µm mesh screens with a sieve shaker before storing in airtight containers for further use, with the <68 and >125 µm fractions corresponding to the recycled catalyst and solid residue, respectively. The weight of each fraction was recorded and adjusted for solids lost during the screening process due to solids transfer. The calcined recycled catalyst was placed in a muffle furnace at 450 °C for 6 h.

The elemental composition of the solid residue (C, H, N, S and O) was determined as the average value (triple repetition) using an elemental Vario MacroCube CHNS analyser, where the % of O was indirectly calculated as complementary percentage to the sum of each element's percentage and the ash content. The dry matter fraction in total solids (TS) was determined by drying at 105 °C until constant weight, while the organic volatile solids (VS) fraction and ash content were determined by combustion at 450 °C for 6 h as % of TS, according to [41,42]. EDX, SEM and BET analyses were conducted using the same methods as the catalyst's characterisation. The crystallinity index was calculated using the peak height method [43].

3. Results and Discussion

3.1. Effects of Process Variables on LA Production

The SZR catalyst was initially investigated for the conversion of biomass to LA with deionised water between 140 and 200 °C for 60–120 min, as shown in Figure 2. The highest

LA yield was 32% at 160 °C for 1 h in aqueous solution which was less than the literature LA yields with a similar sulphated catalyst with microcrystalline cellulose [44]. In this study, there was a negligible yield of a key intermediate of LA production, 5-HMF, which was previously reported as the bottleneck by Kassaye et al. with a similar sulphated zirconium [44]. Other zirconium-based catalysts with zirconia and zirconium phosphate reported LA yields of 53.9% and 52.9%, respectively, from microcrystalline cellulose with deionised water [24,45]. The reported yields in this study indicate that the heterogeneity and physical complexity of real lignocellulose reduce the solid–solid interaction compared with microcrystalline cellulose and are the cause of the decrease in LA between this study and the literature.

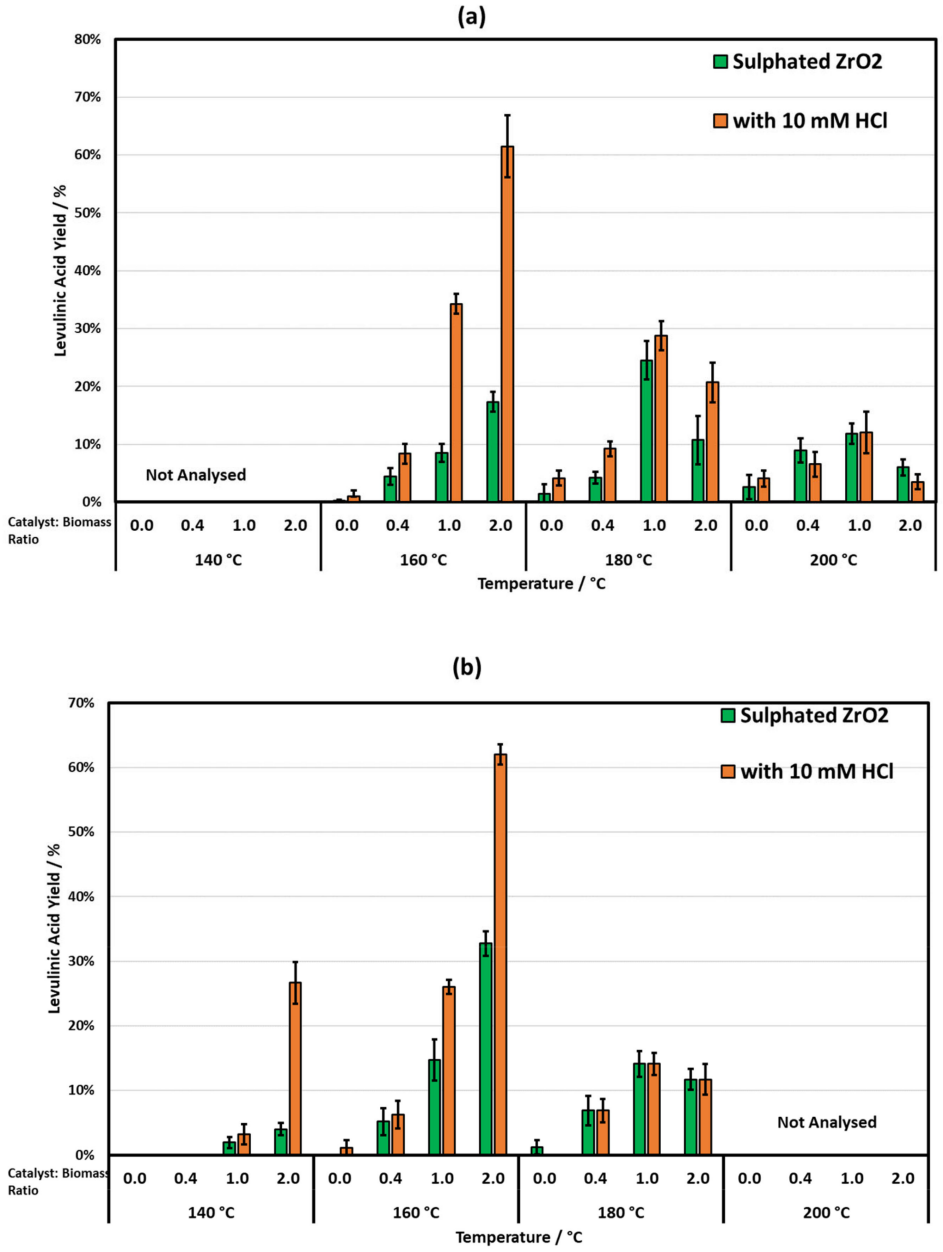

Figure 2. LA yield from SZR catalysis of *Miscanthus x Giganteus* in 10 mL of water or 10 mM HCl with varying catalyst-to-biomass ratios for (**a**) 60 min; (**b**) 120 min.

The addition of trace HCl drastically increased the LA yields under nearly all conditions, achieving a 61.5% LA yield at 160 °C for 1 h with a catalyst-to-biomass ratio of 2:1. This yield is comparable with the commercialised Biofine process, which achieved a 67%

LA yield using H_2SO_4 catalysts with similar *Miscanthus x Giganteus* [3]. The increase in LA yields could be attributed to the increased efficiency of SZR due to the acidic medium or a direct effect of trace HCl on biomass conversion towards oligosaccharides. The use of 10 mM HCl in the absence of SZR exhibited low LA yields of below 5% under all conditions, showing that trace HCl had minimal direct effect other than synergism with the sulphated zirconium. Oligosaccharides and monosaccharides were not measured in this study; however, it may be possible that the trace HCl at such low quantities is acting as a simultaneous pre-treatment alongside the SZR catalysis [27]. The LA yields increased significantly with increasing catalyst-to-biomass ratio up to 2:1, below 160 °C. This clearly suggests that the SZR is the primary catalyst compared to the dilute hydrochloric acid, and higher catalyst ratios could yield further benefits. However, a catalyst-to-biomass ratio beyond 2:1 was not investigated due to slurry issues with such high solids loading in the reactor configuration.

There was a noticeable reduction in LA yields with increasing catalyst-to-biomass ratio from 1 to 2 at temperatures exceeding 180 °C. This suggests that at higher temperatures, SZR could be catalysing the degradation of LA or high-temperature humin formation is partially deactivating the catalyst. Most promisingly, the effect of dilute HCl at 140 °C showed a remarkable increase from 3.0% to 26.6%, despite the low-temperature conversion of cellulose being notoriously difficult. This improvement may be indicative of the potential heterogeneous catalyst synergy with aqueous ions for low-temperature biomass catalysis and should be explored further.

The reaction parameters (time, temperature and catalyst-to-biomass ratio) were further optimised using the response surface methodology (RSM), detailed in Supplementary Tables S1–S4 and Supplementary Figure S1. The optimisation of the HCl–SZR ratio with regard to optimised Lewis–Brønsted acid was not considered in the study as the focus was the investigation of SZR. The highest predicted LA yield was predicted at approximately 160 °C for 80 min, which upon further investigation was found to result in a 63.8% LA yield. As the optimised reactions conditions resulted in the highest product yields, these conditions were chosen for the investigation of catalyst recyclability and solid residue characteristics.

3.2. Catalyst Characterisation and Recyclability

The sulphation of zirconium dioxide resulted in the surface modification shown in Figure 3a,b, whilst the calcinated versus non-calcinated catalyst comparison for recyclability is supplied in Figure S2. The XRD pattern, Figure 3c, shows the presence of the tetragonal phase of zirconium dioxide, given by the reflections at 31°, 50° and 60° two theta, which closely corresponds with the previously reported literature [46]. The surface composition was analysed using EDX, Figure 3d, and revealed a high degree of sulphation was achieved with a surface sulphur content of 4.0 wt.%., which is directly responsible for the levels of acidity during the reaction. This suggests a significant increase in the surface acidity compared to the uncoated ZrO_2. The BET surface area, shown in Table 1, was measured at 72 m^2/g with a significant external surface area of 53 m^2/g and presence of mesopores (supplementary Figures S3 and S4) available for cellulose hydrolysis. The NH_3-TPD acidity of fresh SZR was measured to be 0.47 mmol/g (Figure S5), which is comparable with other works with sulphated zirconias [24,47].

The catalyst recyclability is of utmost importance for the low-cost application production of LA with solid acid catalysts. The solid acid catalyst was mechanically separated from the solid residue through a 68 µm sieve which resulted in a 63% catalyst recovery (excluding 12% vs. catalyst contamination). The effects of calcination at 450 °C on catalyst reusability were investigated to understand both the possible catalyst deactivation mechanisms and to evaluate possible non-calcined catalyst recovery processes.

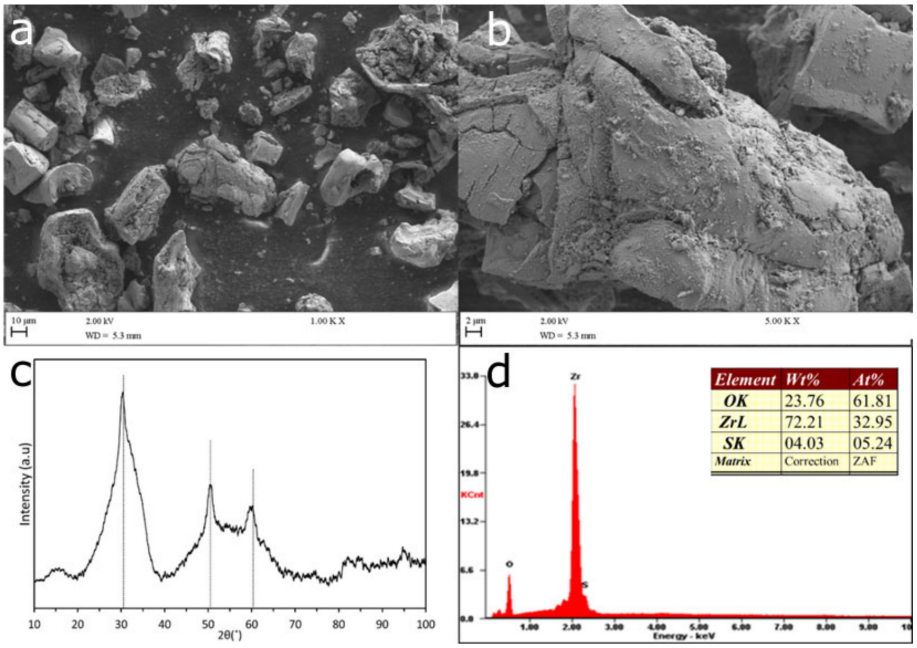

Figure 3. (**a**,**b**) SEM images of SZR catalyst; (**c**) XRD pattern of SZR; (**d**) EDX of SZR.

Table 1. BET surface area (S_{BET}), total pore volume (V_{TOTAL}), micropore volume (V_{MICRO}), external surface area (S_{EXT}) and average pore size (D) (calculated from the BET surface area and the total pore volume assuming cylindrical pores ($D = 4V_{TOTAL}/S_{BET}$)) of Raw SZR and Solid Residue.

Sample	S_{BET} ($m^2\ g^{-1}$)	V_{TOTAL} ($cm^3\ g^{-1}$)	V_{MICRO} ($cm^3\ g^{-1}$)	S_{EXT} ($m^2\ g^{-1}$)	D (nm)
Raw SZR	72	0.10	0.009	53	5.6
Solid Residue	23	0.11	0.005	13	19.9

Figure 4 shows the reuse of SZR over three consecutive cycles with (calcinated) and without (uncalcinated) further calcination after the initial thermal treatments described in Section 2.1. The non-calcined SZR experienced a significant drop in LA yields to 25.5% at the third cycle compared with a 42.3% yield with the calcined catalyst. The EDX analysis of the recycled catalysts (Figure S2) shows that the uncalcined catalyst surface has a higher surface carbon content (28.6 wt.%) compared to the calcined catalyst (20.4 wt.%). The increase in the surface carbon content suggests the adsorption of humins and other carbonaceous residues that are thermally stable at 450 °C. Higher-temperature calcination may further reduce the carbon content; however, others studies have found that synthetic humins are thermally robust at higher temperatures with only a 66 wt.% decomposition at 1000 °C [34]. It should also be noted that there was a decrease in the surface sulphur content (1.73–1.95%) compared to 4.3 wt.% in the fresh catalyst, which indicates possible de-sulphation of the catalyst by the trace HCl or selective poisoning of the sulphate groups by humin formation. The amount of Zr leaching due to the presence of HCl was determined using ICP to be <0.1% (Supplementary Table S3), which is comparable to other works using zirconium in deionised water [24]. The deactivation of solid acid catalysts by humin formation can be controlled by the residence time of the reactor which can be partially achieved using continuous reactors [48]. Porous solid acid ZSM-5 has recently been found to be an effective pyrolysis catalyst for synthetic humins at 550 °C [49], as well as a potential catalyst for levulinic acid [18]. Han et al. suggested that solid acid catalysts can catalyse the degradation of lignin-like residues; however, a porous catalyst structure is required to prevent repolymerisation of intermediaries towards char [50]. Moreover, as the minimisation of humin formation is difficult, future work should consider solid

catalysts that catalytically degrade the humin residue during calcination or pyrolysis for the development of a more reusable catalyst.

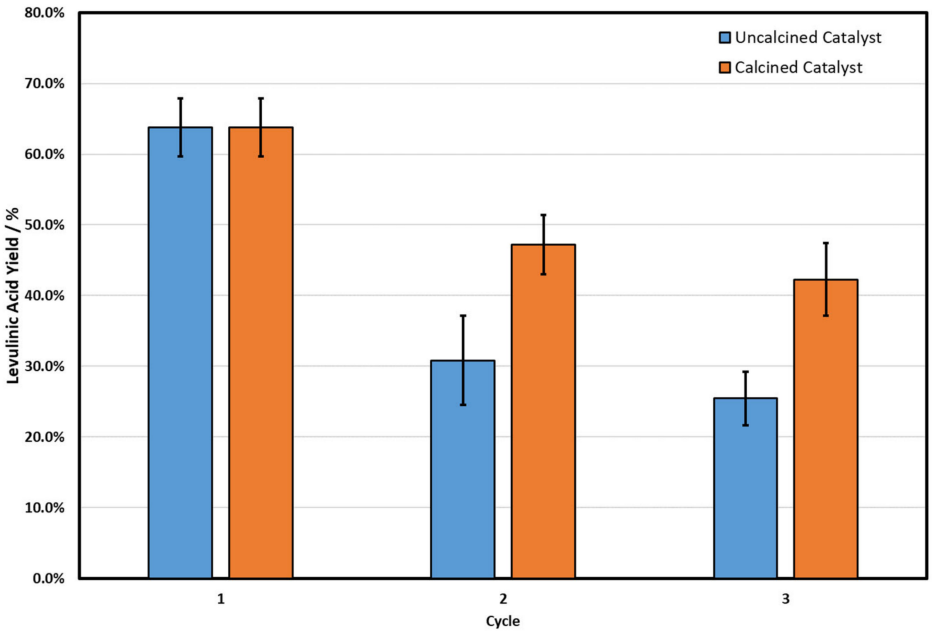

Figure 4. Reusability of the SZR catalyst using uncalcined and calcined at 450 °C catalysts with 0.25 g of *Miscanthus x Giganteus* in 10 mL of 10 mM HCl at 160 °C at 80 min with a 2:1 catalyst-to-biomass ratio.

3.3. Solid Residue Characterisation and Possible Applications

The SR weights after each trial were determined assuming no catalyst leaching. The catalyst and solid residue were separated by sieving and correspond to <63 and >125 µm, respectively. The >125 µm fraction contained approximately 21% ZrO_2, as identified using XRF and shown in Table 2, indicating significant catalyst contamination despite the high SR separation yield, 79 wt.%. However, on the industrial scale, the catalyst—solid residue—separation can be carried out using more efficient methods such as froth flotation; therefore, as the >125 µm fraction is predominately SR, it can be used to evaluate SR properties.

Table 2. Material characterisation of separated solid residue produced during the optimum conditions of 160 °C for 80 min with a 2:1 catalyst-to-biomass ratio.

	Value
Estimated SR Sep. Yield/wt.%	79.0%
ZrO2 content/wt.%	21%
Ash/%	36.3%
ZrO2 adjusted Ash/wt.%	14.9%
C/wt.%	36.8%
H/wt.%	4.3%
O/wt.%	20.2%
C/N	134.00
H/C	1.40
O/C	0.42
HHV */MJ kg^{-1}	16.2

* $HHV_{predicted}$ = 0.3491(C) + 1.1783(H) + 0.1005(N) − 0.1034(O) − 0.0015(A), where C, H, S, O and A represent the weight percentages of carbon, hydrogen, sulphur, oxygen and ash of the sample, respectively [51].

The SR produced during the catalysis with and without the addition of 10 mM HCl was analysed using X-ray diffraction (XRD) and compared with the raw biomass, as shown in Figure 5. The relative crystallinity of the raw biomass, solid residue from SZR in water

medium and 10 mM HCl catalysis was 77.8%, 88.3% and 93.5%, respectively. This strongly suggests that the SZR favourably removes amorphous cellulose, which is in agreement with the effects of other solid acid catalysts in the literature [52]. The addition of 10 mM HCl significantly increases the degradation of amorphous cellulose compared to the water medium, which could be indicative of the role of trace HCl in cellulose depolymerisation. However, the crystallinity index is a relative ratio that cannot determine the absolute effect on both cellulose fractions.

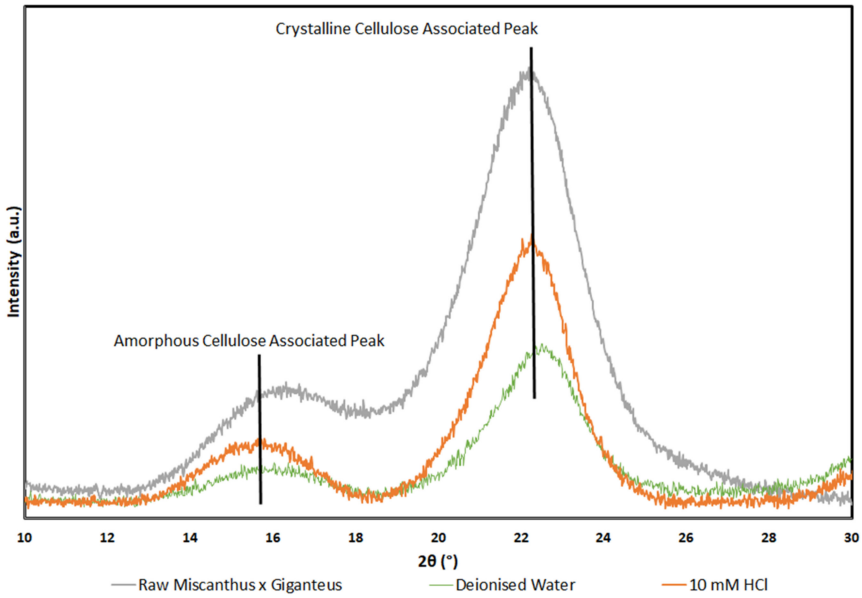

Figure 5. XRD pattern of raw *Miscanthus x Giganteus* and solid residue produced in deionised water and 10 mM HCl with a 2:1 catalyst-to-biomass ratio at 180 °C for 60 min.

Throughout the work, it is observed that increased catalyst ratios resulted in lower SR yields, and this was especially significant when dilute HCl was added to the reaction medium. At the validated optimum point identified by the RSM model (Supplementary Figure S1), corresponding to 160 °C, 80 min and a 2:1 catalyst-to-biomass ratio with 10 mM dilute HCl, the SR yield was about 58–62 wt.%. The compositional properties of the residues at the optimum point are reported in Table 2. The initially high ash content (36.3%) can be attributed to the catalyst contamination, although the ZrO_2 adjusted ash content is still considerably high (14.9%), exceeding previously reported ash contents of other residues. This may indicate that the mild acidic conditions do not extract acid-soluble elements during the process unlike concentrated sulphuric acid, resulting in a higher ash content in the residue. However, the high C/N ratio limits the application of the residue as a soil fertiliser, despite the increase in trace mineral elements. After the catalysis process, the H/C and O/C ratios decreased compared with the raw feedstock, as shown in Supplementary Figure S6. The relative decrease in both H/C and O/C strongly indicates that the feedstock primarily underwent hydrolysis as expected with an acid hydrolysis process. The resulting SR elemental composition was similar to hydrochars produced under non-acidic conditions and could suggest similar applications to that of hydrochars [53].

In order to understand the effect of humin formation compared to homogenous catalysts, the SR from the optimum conditions was compared to BIOFINE-like conditions previously investigated by our group, using SEM, as shown in Figure 6. It can be clearly seen how the carbonaceous spheres (humins) do not form when the reaction runs at the optimum conditions identified by the RSM model. We think the catalyst type is mainly responsible for this phenomenon, as the solid–solid interaction bottleneck for cellulose hydrolysis previously discussed also applies to humin formation. The heterogeneous catalyst reduces the number of active sites available for humin formation and humin growth by aldol polymerization. This was evident in all RSM combinations tested (non-

optimum) which confirms this outcome, as there was no significant increase in residue yields at extreme conditions, indicating a minimal solid by-product-forming reaction, where humin deposition appears to shift from the residue towards the catalyst. The lack of structural change from the XRD analysis and lack of an obvious humin solid by-product confirm the previously mentioned high H/C and O/C ratios. This makes it obvious that the solid residue using sulphated catalysts, and possibly most heterogeneous catalysts, is more akin to the degraded biomass than the chars produced using homogenous catalysts such as sulphuric acid (Biofine process).

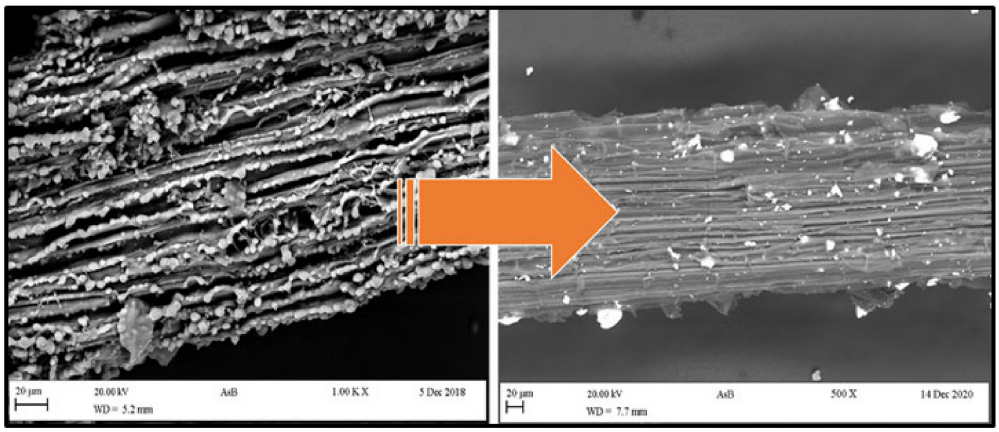

Figure 6. Humin deposition on solid residue (SR) between Biofine-like (on the left) and optimum RSM (on the right) conditions.

This significant change in SR by-products will have stark commercial implications for the overall acid catalysis process. Previous studies have looked at harnessing the char-like properties of SR from LA production as a solid fuel or feedstock for pyrolysis. The higher heating value (HHV) was estimated to be 16.2 MJ kg^{-1}, as shown in Table 2, which suggests a possible use as a solid fuel. The increased ash content will, however, significantly reduce the combustion properties. Further, the HHV is significantly lower than the raw feedstock, other hydrochars and synthetic humins, 22, 20–29 and 21–24 MJ kg^{-1}, respectively [34,53]. A more appropriate application could possibly be as a soil amendment to increase soil carbon content and fertility. As previously mentioned, the increased ash and thus mineral contents of the SR could possibly increase the soil buffering capacity as well as providing a supply of available nutrients to promote microbial growth. The modest surface area of 23 m^2 g^{-1} with the presence of larger pores (Table 1 and supplementary Figures S3 and S4) could also potentially promote microbial growth, and the presence of undigested cellulose will provide an energy source for rapid microbial colonisation without the requirement of an extra food source. However, the applicability of the SR as a soil amendment will require further field investigation due to the complex nature of soil amendments.

4. Conclusions

The results from this study indicate that microwave-assisted conversion of lignocellulosic biomass to levulinic acid using sulphated zirconia and trace hydrochloric acid is a promising method. The performed lab-scale experiments showed that an optimum yield of about 63% wt. can be achieved at 160 °C, 80 min and a 2:1 catalyst-to-biomass ratio with 10 mM dilute HCl. The synergistic performance of the sulphated zirconia and hydrochloric acid significantly improved levulinic acid yields compared with that of each individual catalyst. This approach could be applied to a range of heterogeneous catalysts to improve product yields with real lignocellulosic biomass. Further work is required to optimise the trace HCl-to-heterogeneous catalyst ratio, with special regard to the Lewis–Brønsted acid ratio, which may facilitate significant progress in the area of heterogeneous catalysis of real biomass. The solid residue was primarily composed of unreacted biomass and did not undergo any significant transformation, suggesting that heterogeneous catalysis of

biomass results in a significant residue compared to that of homogenous catalysts with different possible commercial applications. The development of this catalyst and synergistic approach could significantly reduce catalyst separation costs with minimal effect on the product yields, which will potentially result in the wide-scale commercialization of low-carbon biofuels and biochemicals.

Supplementary Materials: The following are available online at https://www.mdpi.com/1996-1073/14/6/1582/s1, Figure S1: 3D response surface plots and 2D contour plots of levulinic acid yield (wt.%) whist (A) varying time and temperature; (B) varying catalyst-to-biomass ratio and temperature; (C) varying catalyst-to-biomass ratio and time, Figure S2: EDX pattern of (a) uncalcined catalyst and (b) calcined catalyst after 3 catalysis cycles with Miscanthus x Giganteus at 180 °C for 80 min with a 2:1 catalyst-to-biomass ratio in 10 mM HCl, Figure S3: Nitrogen adsorption–desorption isotherms of the residue and the sulphated zirconia catalyst, Figure S4: BJH adsorption pore size distributions of the residue and the sulphated zirconia catalyst, Figure S5: Ammonia TPD of fresh sulphated zirconia catalyst, Figure S6: Van Krevelen diagram of raw Miscanthus x Giganteus and produced solid residue, Table S1: Levels of independent variables, Table S2: Raw Data for RSM predicted yields, Table S3: ANOVA of proposed model for Levulinic acid yield—right-hand side is updated model after removing insignificant terms (R^2 = 93.70%, adj-R^2 = 87.40%, predicted R^2 = 0.5384), Table S4: Catalyst recyclability based on post-reaction Zr(IV) leaching.

Author Contributions: Project conceptualization, S.T.; catalyst preparation and design, J.M.G.-C.; catalyst characterization, J.M.G.-C., G.H. and L.T.; biomass catalysis and data collection, G.H.; writing—original draft preparation, G.H. and S.T.; writing—review and editing, J.M.G.-C., L.T. and S.T.; supervision, S.T.; funding acquisition, S.T. All authors have read and agreed to the published version of the manuscript.

Funding: This research was funded by the EPSRC's SUPERGEN Bioenergy Hub via the Rapid Response Scheme (RR 2020_4).

Institutional Review Board Statement: Not applicable.

Informed Consent Statement: Not applicable.

Data Availability Statement: All data generated by this study is contained within this article and the attached supplementary material.

Acknowledgments: We would like to acknowledge and thank the industry partners, Drochaid Research Services Ltd., St Andrews, UK (Bob Tooze and Juan Maria Gonzalez-Carballo), for their invaluable contribution to this project in terms of consultancy and resources.

Conflicts of Interest: The authors declare no conflict of interest.

References

1. Sweygers, N.; Dewil, R.; Appels, L. Production of Levulinic Acid and Furfural by Microwave-Assisted Hydrolysis from Model Compounds: Effect of Temperature, Acid Concentration and Reaction Time. *Waste Biomass Valoriz.* **2018**, *9*, 343–355. [CrossRef]
2. Signoretto, M.; Taghavi, S.; Ghedini, E.; Menegazzo, F. Catalytic Production of Levulinic Acid (LA) from Actual Biomass. *Molecules* **2019**, *24*, 2760. [CrossRef] [PubMed]
3. Dussan, K.; Girisuta, B.; Haverty, D.; Leahy, J.J.; Hayes, M.H.B. Bioresource Technology Kinetics of levulinic acid and furfural production from Miscanthus Â giganteus. *Bioresour. Technol.* **2013**, *149*, 216–224. [CrossRef] [PubMed]
4. Werpy, T.; Petersen, G. *Top Value Added Chemicals from Biomass Volume I*; National Renewable Energy Lab.: Golden, CO, USA, 2004; 76p.
5. Acharjee, T.C.; Lee, Y.Y. Production of levulinic acid from glucose by dual solid-acid catalysts. *Environ. Prog. Sustain. Energy* **2018**, *37*, 471–480. [CrossRef]
6. Girisuta, B.; Janssen, L.P.B.M.; Heeres, H.J. Kinetic study on the acid-catalyzed hydrolysis of cellulose to levulinic acid. *Ind. Eng. Chem. Res.* **2007**, *46*, 1696–1708. [CrossRef]
7. Xue, Z.; Yu, D.; Zhao, X.; Mu, T. Upgrading of levulinic acid into diverse N-containing functional chemicals. *Green Chem.* **2019**, *21*, 5449–5468. [CrossRef]
8. Licursi, D.; Antonetti, C.; Fulignati, S.; Giannoni, M.; Raspolli Galletti, A.M. Cascade strategy for the tunable catalytic valorization of levulinic acid and γ-valerolactone to 2-methyltetrahydrofuran and alcohols. *Catalysts* **2018**, *8*, 277. [CrossRef]
9. Xie, Z.; Chen, B.; Wu, H.; Liu, M.; Liu, H.; Zhang, J.; Yang, G.; Han, B. Highly efficient hydrogenation of levulinic acid into 2-methyltetrahydrofuran over Ni–Cu/Al2O3–ZrO2 bifunctional catalysts. *Green Chem.* **2019**, *21*, 606–613. [CrossRef]

10. Zheng, X.; Zhi, Z.; Gu, X.; Li, X.; Zhang, R.; Lu, X. Kinetic study of levulinic acid production from corn stalk at mild temperature using FeCl3 as catalyst. *Fuel* **2017**, *187*, 261–267. [CrossRef]
11. Di Fidio, N.; Fulignati, S.; De Bari, I.; Antonetti, C.; Raspolli Galletti, A.M. Optimisation of glucose and levulinic acid production from the cellulose fraction of giant reed (Arundo donax L.) performed in the presence of ferric chloride under microwave heating. *Bioresour. Technol.* **2020**, *313*, 123650. [CrossRef]
12. Bozell, J.J.; Moens, L.; Elliott, D.C.; Wang, Y.; Neuenscwander, G.G.; Fitzpatrick, S.W.; Bilski, R.J.; Jarnefeld, J.L.; Northwest, P.; Box, P.O.; et al. Production of levulinic acid and use as a platform chemical for derived products. *Resour. Conserv. Recycl.* **2000**, *28*, 227–239. [CrossRef]
13. Leal Silva, J.F.; Grekin, R.; Mariano, A.P.; Maciel Filho, R. Making Levulinic Acid and Ethyl Levulinate Economically Viable: A Worldwide Technoeconomic and Environmental Assessment of Possible Routes. *Energy Technol.* **2018**, *6*, 613–639. [CrossRef]
14. Gozan, M.; Ryan, B.; Krisnandi, Y. Techno-economic assessment of Levulinic Acid Plant from Sorghum Bicolor in Indonesia. In Proceedings of the 2nd International Conference on Oleo and Petrochemical Engineering (ICOOPChE 2017), Pekanbaru-Riau, Indonesia, 29–30 November 2017; Volume 345.
15. Leal Silva, J.F.; MacIel Filho, R.; Wolf MacIel, M.R. Process Design and Technoeconomic Assessment of the Extraction of Levulinic Acid from Biomass Hydrolysate Using n-Butyl Acetate, Hexane, and 2-Methyltetrahydrofuran. *Ind. Eng. Chem. Res.* **2020**, *59*, 11031–11041. [CrossRef]
16. Van De Vyver, S.; Thomas, J.; Geboers, J.; Keyzer, S.; Smet, M.; Dehaen, W.; Jacobs, P.A.; Sels, B.F. Catalytic production of levulinic acid from cellulose and other biomass-derived carbohydrates with sulfonated hyperbranched poly(arylene oxindole)s. *Energy Environ. Sci.* **2011**, *4*, 3601–3610. [CrossRef]
17. Weingarten, R.; Conner, W.C.; Huber, G.W. Production of levulinic acid from cellulose by hydrothermal decomposition combined with aqueous phase dehydration with a solid acid catalyst. *Energy Environ. Sci.* **2012**, *5*, 7559–7574. [CrossRef]
18. Pratama, A.P.; Rahayu, D.U.C.; Krisnandi, Y.K. Levulinic acid production from delignified rice husk waste over manganese catalysts: Heterogeneous versus homogeneous. *Catalysts* **2020**, *10*, 327. [CrossRef]
19. Wang, P.; Zhan, S.; Yu, H. Production of Levulinic Acid from Cellulose Catalyzed by Environmental-Friendly Catalyst. *Adv. Mater. Res.* **2010**, *96*, 183–187. [CrossRef]
20. Ya'Aini, N.; Amin, N.A.S.; Endud, S. Characterization and performance of hybrid catalysts for levulinic acid production from glucose. *Microporous Mesoporous Mater.* **2013**, *171*, 14–23. [CrossRef]
21. Peixoto, A.F.; Silva, S.M.; Costa, P.; Santos, A.C.; Valentim, B.; Lázaro-Martínez, J.M.; Freire, C. Acid functionalized coal fly ashes: New solid catalysts for levulinic acid esterification. *Catal. Today* **2020**, *357*, 74–83. [CrossRef]
22. Antonetti, C.; Licursi, D.; Fulignati, S.; Valentini, G.; Maria, A.; Galletti, R. New Frontiers in the Catalytic Synthesis of Levulinic Acid: From Sugars to Raw and Waste Biomass as Starting Feedstock. *Catalysts* **2016**, *6*, 196. [CrossRef]
23. Lappalainen, K.; Vogeler, N.; Kärkkäinen, J.; Dong, Y.; Niemelä, M.; Rusanen, A.; Ruotsalainen, A.L.; Wäli, P.; Markkola, A.; Lassi, U. Microwave-assisted conversion of novel biomass materials into levulinic acid. *Biomass Convers. Biorefin.* **2018**, *8*, 965–970. [CrossRef]
24. Joshi, S.S.; Zodge, A.D.; Pandare, K.V.; Kulkarni, B.D. Efficient conversion of cellulose to levulinic acid by hydrothermal treatment using zirconium dioxide as a recyclable solid acid catalyst. *Ind. Eng. Chem. Res.* **2014**, *53*, 18796–18805. [CrossRef]
25. Qi, X.; Watanabe, M.; Aida, T.M.; Smith, R.L. Sulfated zirconia as a solid acid catalyst for the dehydration of fructose to 5-hydroxymethylfurfural. *Catal. Commun.* **2009**, *10*, 1771–1775. [CrossRef]
26. Pyo, S.H.; Glaser, S.J.; Rehnberg, N.; Hatti-Kaul, R. Clean Production of Levulinic Acid from Fructose and Glucose in Salt Water by Heterogeneous Catalytic Dehydration. *ACS Omega* **2020**, *5*, 14275–14282. [CrossRef]
27. Kobayashi, H.; Kaiki, H.; Shrotri, A.; Techikawara, K.; Fukuoka, A. Hydrolysis of woody biomass by a biomass-derived reusable heterogeneous catalyst. *Chem. Sci.* **2016**, *7*, 692–696. [CrossRef] [PubMed]
28. Geboers, J.; Van de Vyver, S.; Carpentier, K.; Jacobs, P.; Sels, B. Hydrolytic hydrogenation of cellulose with hydrotreated caesium salts of heteropoly acids and Ru/C. *Green Chem.* **2011**, *13*, 2167–2174. [CrossRef]
29. Lopes, E.S.; Leal Silva, J.F.; Rivera, E.C.; Gomes, A.P.; Lopes, M.S.; Maciel Filho, R.; Tovar, L.P. Challenges to Levulinic Acid and Humins Valuation in the Sugarcane Bagasse Biorefinery Concept. *Bioenergy Res.* **2020**, *13*, 757–774. [CrossRef]
30. Patil, S.K.R.; Lund, C.R.F. Formation and Growth of Humins via Aldol Addition and condensation during acid-catalyzed conversion of 5-hydroxymethylfurfural. *Energy Fuels* **2011**, *25*, 4745–4755. [CrossRef]
31. Zandvoort, I.V.; Wang, Y.; Rasrendra, C.B.; Eck, E.R.H.V.; Bruijnincx, P.C.A.; Heeres, H.J.; Weckhuysen, B.M. Formation, Molecular Structure, and Morphology of Humins in Biomass Conversion: Influence of Feedstock and Processing Conditions. *ChemSusChem* **2013**, *6*, 1745–1758. [CrossRef] [PubMed]
32. Peeters, G.H.I.B.M.; Tedesco, S. Solid residue and by—Product yields from acid—Catalysed conversion of poplar wood to levulinic acid. *Chem. Pap.* **2020**, *74*, 1647–1661.
33. Hayes, D.J.; Fitzpatrick, S.; Hayes, M.H.B.; Ross, J.R.H. The Biofine Process—Production of Levulinic Acid, Furfural, and Formic Acid from Lignocellulosic Feedstocks. In *Biorefineries-Industrial Processes and Products: Status Quo and Future Directions*; Kanm, B., Gruber, P.R., Kamm, M., Eds.; WILEY-VCH Verlag GmbH & Co. KGaA: Weinheim, Germany, 2006.
34. Agarwal, S.; Van Es, D.; Heeres, H.J. Catalytic pyrolysis of recalcitrant, insoluble humin byproducts from C6 sugar biorefineries. *J. Anal. Appl. Pyrolysis* **2017**, *123*, 134–143. [CrossRef]

35. Melligan, F.; Dussan, K.; Auccaise, R.; Novotny, E.H.; Leahy, J.J.; Hayes, M.H.B.; Kwapinski, W. Bioresource Technology Characterisation of the products from pyrolysis of residues after acid hydrolysis of Miscanthus. *Bioresour. Technol.* **2012**, *108*, 258–263. [CrossRef] [PubMed]
36. Mija, A.; Van Der Waal, J.C.; Pin, J.; Guigo, N.; De Jong, E. Virtual Special Issue Bio Based Building Materials Humins as promising material for producing sustainable carbohydrate-derived building materials. *Constr. Build. Mater.* **2017**, *139*, 594–601. [CrossRef]
37. Lehmann, J.; Joseph, S. *Biochar for Environmental Management*; EarthScan: London, UK, 2012; ISBN 9781844076581.
38. Nielsen, S.; Minchin, T.; Kimber, S.; van Zwieten, L.; Gilbert, J.; Munroe, P.; Joseph, S.; Thomas, T. Comparative analysis of the microbial communities in agricultural soil amended with enhanced biochars or traditional fertilisers. *Agric. Ecosyst. Environ.* **2014**, *191*, 73–82. [CrossRef]
39. Solaiman, Z.M.; Anawar, H.M. Application of Biochars for Soil Constraints: Challenges and Solutions. *Pedosphere* **2015**, *25*, 631–638. [CrossRef]
40. McCalmont, J.P.; Hastings, A.; McNamara, N.P.; Richter, G.M.; Robson, P.; Donnison, I.S.; Clifton-Brown, J. Environmental costs and benefits of growing Miscanthus for bioenergy in the UK. *Gcb Bioenergy* **2017**, *9*, 489–507. [CrossRef]
41. Sluiter, A.; Hames, B.; Hyman, D.; Payne, C.; Ruiz, R.; Scarlata, C.; Sluiter, J.; Templeton, D.; Wolfe, J. Determination of total solids in biomass and total dissolved solids in liquid process samples. Laboratory Analytical Procedure (LAP). *Natl. Renew. Energy Lab.* **2008**, *9*, 1–6.
42. Ehrman, T. *Standard Method for Ash in Biomass*; Laboratory Analytical Procedure-005, National Renewable Energy Laboratory, Midwest Research Institute for the Department of Energy: Golden, Colorado, 1994.
43. Park, S.; Baker, J.O.; Himmel, M.E.; Parilla, P.A.; Johnson, D.K. Cellulose crystallinity index: Measurement techniques and their impact on interpreting cellulase performance. *Biotechnol. Biofuels* **2010**, *3*, 1–10. [CrossRef]
44. Kassaye, S.; Pagar, C.; Pant, K.K.; Jain, S.; Gupta, R. Depolymerization of microcrystalline cellulose to value added chemicals using sulfate ion promoted zirconia catalyst. *Bioresour. Technol.* **2016**, *220*, 394–400. [CrossRef]
45. Ding, D.; Wang, J.; Xi, J.; Liu, X.; Lu, G.; Wang, Y. High-yield production of levulinic acid from cellulose and its upgrading to γ-valerolactone. *Green Chem.* **2014**, *16*, 3846–3853. [CrossRef]
46. Muthu, H.; Selvabala, V.S.; Varathachary, T.K.; Selvaraj, D.K.; Nandagopal, J.; Subramanian, S. Synthesis of biodiesel from neem oil using sulfated zirconia via tranesterification. *Braz. J. Chem. Eng.* **2010**, *27*, 601–608. [CrossRef]
47. Yuan, H.; Dong, Z.; He, J.; Wang, Y.; Zhang, H. Surface characterization of sulfated zirconia and its catalytic activity for epoxidation reaction of castor oil. *Chem. Eng. Commun.* **2019**, *206*, 1618–1627. [CrossRef]
48. Pyo, S.H.; Sayed, M.; Hatti-Kaul, R. Batch and Continuous Flow Production of 5-Hydroxymethylfurfural from a High Concentration of Fructose Using an Acidic Ion Exchange Catalyst. *Org. Process Res. Dev.* **2019**, *23*, 952–960. [CrossRef]
49. Abdilla-Santes, R.M.; Agarwal, S.; Xi, X.; Heeres, H.; Deuss, P.J.; Heeres, H.J. Valorization of humin type byproducts from pyrolytic sugar conversions to biobased chemicals. *J. Anal. Appl. Pyrolysis* **2020**, *152*, 104963. [CrossRef]
50. Han, T.; Ding, S.; Yang, W.; Jönsson, P. Catalytic pyrolysis of lignin using low-cost materials with different acidities and textural properties as catalysts. *Chem. Eng. J.* **2019**, *373*, 846–856. [CrossRef]
51. Channiwala, S.A.; Parikh, P.P. A unified correlation for estimating HHV of solid, liquid and gaseous fuels. *Fuel* **2002**, *81*, 1051–1063. [CrossRef]
52. Di Fidio, N.; Galletti, A.M.R.; Fulignati, S.; Licursi, D.; Liuzzi, F.; De Bari, I.; Antonetti, C. Multi-step exploitation of raw arundo donax L. For the selective synthesis of second-generation sugars by chemical and biological route. *Catalysts* **2020**, *10*, 79. [CrossRef]
53. Kambo, H.S.; Dutta, A. A comparative review of biochar and hydrochar in terms of production, physico-chemical properties and applications. *Renew. Sustain. Energy Rev.* **2015**, *45*, 359–378. [CrossRef]